APEM journal
Advances in Production Engineering & Management
Volume 11 | Number 2 | June 2016 | pp 93–104
http://dx.doi.org/10.14743/apem2016.2.212
ISSN 1854-6250
Journal home: apem-journal.org
Original scientific paper

Surface roughness assessing based on digital image features

Simunovic, G.[a,*], Svalina, I.[a], Simunovic, K.[a], Saric, T.[a], Havrlisan, S.[a], Vukelic, D.[b]

[a]Mechanical Engineering Faculty in Slavonski Brod, University of Osijek, Croatia
[b]Faculty of Technical Sciences, University of Novi Sad, Serbia

ABSTRACT

The paper gives an account of the machined surface roughness investigation based on the features of a digital image taken subsequent to the technological operation of milling of aluminium alloy Al6060. The data used for investigation were obtained by mixed-level factorial design with two replicates. Input variables (factors) are represented by the face milling basic machining parameters: spindle speed (at five levels: 2000; 3500; 5000; 6500; 8000 rev/min, respectively), feed per tooth (at six levels: 0.025; 0.1; 0.175; 0.25; 0.325; 0.4 mm/tooth, respectively) and depth of cut (at two levels: 1; 2 mm, respectively). Output variable or response is the most frequently used surface roughness parameter – arithmetic average of the roughness profile, *Ra*. Digital image of the machined surface is provided for every test sample. Based on experimental design and obtained results of roughness measuring, a base has been created of input data (features) extracted from digital images of the samples' machined surfaces. This base was later used for generating the fuzzy inference system for prediction of the surface roughness using the adaptive neuro-fuzzy inference system (ANFIS). Assessing error, i.e. comparison of the assessed value *Ra* provided by the system with real *Ra* values, is expressed with the normalized root mean square error (NRMSE) and it is 0.0698 (6.98 %).

ARTICLE INFO

Keywords:
Surface roughness
Face milling
Digital image
Adaptive neuro-fuzzy inference system

**Corresponding author:*
goran.simunovic@sfsb.hr
(Simunovic, G.)

Article history:
Received 7 March 2016
Revised 15 May 2016
Accepted 16 May 2016

1. Introduction

Surface roughness is an important technological parameter and indicator of the machined surface quality. Requirements for lower values of surface roughness simultaneously affect the prolongation of machining time and increase of production costs. Surface roughness is conditioned by a larger number of controlled and uncontrolled process parameters (including cutting speed, depth of cut and feed rate, raw material properties, cutting conditions, tool properties, tool machine vibrations, tool wear etc.). By regular monitoring the results of a machining process and expanding the knowledge base about the monitored parameters of observed processes, it is possible to continuously improve a product characteristic and production results.

There is a great number of scientific investigations aimed at prediction and control of surface roughness [1-4]. The models defined in these investigations can be divided into regression (statistic), analytic (mathematic) and those based on the application of artificial intelligence (AI) [5-8].

It is often the case that the digital image features of the machined surfaces are used in controlling or assessing the machined surface roughness. The image features are used as input variables for the assessing model [9-13], and they are mostly represented by statistic values such as arithmetic mean and standard deviation [14], different kinds of standards such as the Euclidean and the Hamming norm [15], wave transformations such as the Haar wavelet transform [16] and

the two-dimensional Fourier transform [17] etc. Adaptive neuro-fuzzy inference system (ANFIS), artificial neural networks (ANN), regression analysis and others are the methods mostly used for assessing.

Lee et al. [14] propose a method using an adaptive neuro-fuzzy inference system (ANFIS) to establish the relationship between actual surface roughness and texture features of the surface image. The input parameters of a training model are spatial frequency, arithmetic mean value, and standard deviation of grey levels from the surface image. In paper [18] the ANFIS is also used in assessing the surface roughness using cutting parameters (cutting speed, feed rate, and depth of cut) and grey level of the surface image. The assessing model error is less than 4.6 %. In papers [19] and [20] machine vision system is also used integrated with ANFIS. Paper [19] assesses *Ra*, tool wear ratio and metal removal rate in micro-turning process. The assessing error is less than 3.5 %. Investigation in paper [20] is directed to assessment of surface roughness of end milled parts. Using a two dimensional Fourier transform (2D FT) features of image texture are extracted, such as peak frequency, principal component magnitude squared value and the average grey level. The ANFIS and the neural networks methods used in assessing roughness are compared and the assessing errors are very close and less than 2.5 %.

In paper [21] the Euclidean and Hamming distances of the surface images are used for surface recognition. Machined surface images with different values of surface roughness were collected. The base is formed of referent images with known values of surface roughness. The Euclidean and Hamming distances between the tested surface and the referent surface image were used in the base to predict the surface roughness of the unknown surface. Excellent concluding results were obtained and the system is suitable for online surface characterization of machined surfaces. The paper [16] presents methodology based on the extraction of texture features from part surface images in the frequency domain using wavelet transform. One-level Haar wavelet transform is applied to the original surface images. Surface evaluation was accomplished by means of the analysis of grey levels in the vertical detail sub-image of surface images. Experimental results show that the proposed approach achieves error rates between 2.59 % and 4.17 %. Paper [22] is also based on the application of the wavelet transform. Authors apply vision system for acquiring digital images of machined surfaces, analyse the image parameters and connect them with the roughness of the surface machined by turning. The machined surface digital images are described using the one-dimensional digital wavelet transform. The neural networks based system is used for assessing roughness. The testing phase error is a bit more than 5 %. Papers [23, 24] also apply Machine Vision and ANN. In paper [23] they are used to assess *Ra* values using the input obtained from the digital images of inclined surfaces which include optical roughness parameters (major peak frequency, principal component magnitude squared, average power spectrum, central power spectrum percentage, ratio of major axis to minor axis). To improve the quality of the images shadow removal algorithm is used. The high value of the ANN model correlation coefficient (87 %) confirms its applicability. Through computer vision system authors in paper [24] collect features of image texture of machined surface (major peak frequency, principal component magnitude squared value and the standard deviation of grey level and by the application of abductive networks they assess surface roughness of turned parts. The assessment error is around 15 %. Authors in papers [25-27] analyse interconnection between the machined surface texture and the machining time, in other words condition and wear of tools. Authors [25] have investigated the relationship between texture features of the grey-level co-occurrence matrix and the machining time in turning operations. Results of investigation have shown that the error between the actual and the calculated machining time ranges from -4.65 % to 7.79 %. Authors in paper [26] used machine vision technique to detect the condition of tools on the basis of turned surface images using an accurate grey level co-occurrence matrix. In paper [27] authors investigated cutting tool nose wear area and surface roughness of turned parts using machine vision system. They developed an algorithm that uses Wiener filtering and simple thresholding on backlit images in order to reduce the impact of ambient factors (ambient lighting) and vibrations. The developed system roughness assessing error was 10 %. In paper [28] authors investigated connection between surface roughness of AA 6061 alloy end milling and image texture features of milled surface. They used grey level co-occurrence matrix to ex-

tract the image texture features (contrast, homogeneity, correlation and energy). For establishing the relation between surface roughness and image texture the regression analysis is applied. The paper [29] demonstrates that some roughness parameters (*Ra*, *Rq*, *Rv*, *Rt* and *Rz*) can be estimated using only image-extracted features and models, without the knowledge of machining parameters. Authors observe three image texture features of turned surface: gradient factor of surface, average cycle of texture and average grey level. There is a very high correlation between surface roughness and the given features of digital image. Authors in [9] investigated surface lay in the surface roughness evaluation using machine vision. Numerous parameters of digital image are considered such as grey level average, grey level co-occurrence matrix based image quantification parameters (contrast, correlation, energy or uniformity, maximum probability and differential box courting based fractal dimension) of machined surface while changing the angle of taking images. Therefore, it can be concluded that investigations were directed towards building a system (machine vision system) for a quicker and cheaper control, i.e. assessment of the roughness of machined surfaces in real time. The actual paper investigations are an additional contribution for assessing roughness of machined surface based on the features of digital image using the adaptive neuro-fuzzy inference system (ANFIS).

2. Experimental and methodology

2.1 Experimental

Investigation is conducted on the material of samples Al6060 T66 (in accordance with the European norms EN AW-6060 T66 [AlMgSi]). Chemical composition of the alloy Al6060 or EN AW-6060 according to EN 573-3 is given in Table 1.

Mass fraction of other elements can be to the maximum of 0.15 %, and individually 0.05 %. Mechanical and physical properties (at 20 °C) of alloy Al6060 or EN AW-6060 according to EN 755-2 are given in Table 2.

Dimensions of samples are 100 × 60 × 10 mm. Samples (Fig. 1) are machined from flat bars of transverse section 60 × 10 mm.

For face milling of 100 × 60 mm surface vertical CNC milling machine was used produced by HASS type VF-2 and face milling cutter of diameter 40 mm produced by Walter with four cutting inserts (holder mark: F 4042.B.040.Z04.15 and inserts mark: ADMT160608R-F56 WKP35S). The machining was carried out based on CNC programme that repeated the same path of the tool. The following machining parameters were being changed: spindle speed, feed per tooth, and depth of cut in an order defined by the selected mixed-level factorial design. For clamping of samples a hydraulic machine vice Alfa NCO-A was used.

As the applied fuzzy inference system will have three inputs, the suggested factorial design has three factors. By a detailed analysis, considering the total number if input/output experimental data for the training phase and the checking phase of inference system, a mixed-level factorial design was selected. Five spindle speeds (2000; 3500; 5000; 6500; 8000 rev/min, respectively), six feeds per tooth (0.025; 0.1; 0.175; 0.25; 0.325; 0.4 mm/tooth, respectively) and two depths of cut (1; 2 mm, respectively) are used, and two replicates of a mixed-level factorial design are run.

Table 1 Chemical composition of Al6060 according to EN 573-3 (wt%)

Si	Fe	Cu	Mn	Mg	Cr	Zn	Ti
0.3-0.6	0.1-0.3	max 0.1	max 0.1	0.35-0.6	max 0.1	max 0.1	max 0.1

Table 2 Mechanical and physical properties (at 20 °C) of material Al6060 according to EN 755-2

Yield tensile strength, MPa	150	Density, kg/m^3	2700
Ultimate tensile strength, MPa	195	Melting point, °C	585-650
Elongation at break, %	8	Electrical conductivity, mS/m	28-34
Hardness, HB	65	Thermal conductivity, W/mK	200-220
Modulus of elasticity, GPa	70	Coefficient of thermal expansion, 10^{-6}/K	23.4

Fig. 1 Preparation of samples

All other features specific for end milling: tool stepover between neighbour paths, number of passes, total length of paths, are held-constant factors, the same as the Maxol cooling/lubricating fluid produced by Forol d.d., tool (milling cutter) and material of the sample.

2.2 Methodology

Adaptive neuro-fuzzy inference system (ANFIS) method for generating fuzzy inference system requires a set of input/output experimental data. The fuzzy inference system (FIS) has three input variables. In generating FIS the ANFIS method with three membership functions per each input was used. Therefore, 27 different fuzzy rules are used to form the base of fuzzy rules.

For the FIS first row the base of fuzzy rules can be written as:

Rule 1: If x is A_1 and y is B_1 and w is C_1 then z is $f_1(x,y,w)$
Rule 2: If x *is* A_2 and y *is* B_2 and w *is* C_2 then z is $f_2(x,y,w)$
...
Rule 27: If x is A_3 and y *is* B_3 and w is C_3 then z is $f_{27}(x,y,w)$

where x, y and w present ANFIS inputs, A_j, B_j and C_j fuzzy sets, and $f_i(x,y,w)$ is the polynomial first row and represents the output of the first row of Sugeno FIS. The system has adaptive nodes (the sets' parameters that are changeable-adaptive) and fixed nodes (the sets' parameters that are fixed-unchangeable). By arrangement, the nodes outputs are marked as $Q_{l,i}$ where l represents the layer and i the number of nodes.

Five layers are usually used to explain the ANFIS architecture.

Layer 1 contains adaptive nodes. Layer 1 node functions are described as:

$$
\begin{aligned}
Q_{1,i} &= \mu_{A_j}(x)\begin{cases} j = 1\ for\ i = 1,\ldots,9 \\ j = 2\ for\ i = 10,\ldots,18 \\ j = 3\ for\ i = 19,\ldots,27 \end{cases} \\
Q_{1,i} &= \mu_{B_j}(y)\begin{cases} j = 1\ for\ i = 1,2,3,10,11,12,19,20,21 \\ j = 2\ for\ i = 4,5,6,13,14,15,22,23,24 \\ j = 3\ for\ i = 7,8,9,16,17,18,25,26,27 \end{cases} \\
Q_{1,i} &= \mu_{C_j}(w)\begin{cases} j = 1\ for\ i = 1,4,7,\ldots,25 \\ j = 2\ for\ i = 2,5,8,\ldots,26 \\ j = 3\ for\ i = 3,6,9,\ldots,27 \end{cases}
\end{aligned}
\tag{1}
$$

where x, y and w present node inputs, A_j, B_j and C_j linguistic labels and μ_{A_j}, μ_{B_j} and μ_{C_j} membership functions. Membership functions determine the degree in which some variable satisfies a specific rule premise. There are various membership functions. In this paper a bell-shape membership function is applied whose general form can be written as:

$$\mu(x) = \frac{1}{1 + \left(\frac{x - c_i}{a_i}\right)^{b_i}} \quad ; \mu(y) = \frac{1}{1 + \left(\frac{y - c_i}{a_i}\right)^{b_i}} \quad ; \mu(w) = \frac{1}{1 + \left(\frac{w - c_i}{a_i}\right)^{b_i}} \tag{2}$$

where a_i, b_i and c_i are parameters of fuzzy sets.

Layer 2 contains fixed nodes Π. This layer fixed nodes represent multiplication of input signals whose product is the output for each node.

$$Q_{2,i} = \omega_i = \mu_{A_j} \cdot \mu_{B_j} \cdot \mu_{C_j}, \qquad for \ i = 1, \dots, 27 \tag{3}$$

Output ω_i is called the firing strength of a fuzzy rule.

Layer 3 contains fixed nodes N. This layer node functions calculate the ratio of the i-th firing strength of a rule and the firing strength of all rules.

$$Q_{3,i} = \overline{\omega}_i = \frac{\omega_i}{\sum \omega_i}, \ for \ \ i = 1, \dots, 27 \tag{4}$$

Output $\overline{\omega}_i$ is called normalized firing strength of a fuzzy rule.

Layer 4 contains adaptive nodes. This layer node functions are expressed as:

$$Q_{4,i} = \overline{\omega}_i \cdot f_i, \ for \ \ i = 1, \dots, 27 \tag{5}$$

where f_i represents conclusions of fuzzy rules for which is valid:

$$f_i = p_i x + q_i y + r_i w + s_i, \ for \ \ i = 1, \dots, 27 \tag{6}$$

where p_i, q_i, r_i and s_i are called consequent parameters.

Layer 5 contains only one fixed node. Function of this node is to calculate the overall output using:

$$Q_5 = f_{out} = \sum_{i=1}^{27} \overline{\omega}_i \cdot f_i = (\overline{\omega}_i x)p_i + (\overline{\omega}_i y)q_i + (\overline{\omega}_i w)r_i + (\overline{\omega}_i)s_i \tag{7}$$

The arithmetic average of the roughness profile *Ra* can be expressed as:

$$Ra = \sum_{i=1}^{n} \overline{\omega}_i \cdot f_i = \sum_{i=1}^{n} \overline{\omega}_i \left(k_{i0} + k_{i1} \cdot n + k_{i2} \cdot f_z + k_{i3} \cdot a_p\right) \tag{8}$$

where $k = [k_{10}, k_{11}, k_{12}, k_{13}, k_{20}, k_{21}, k_{22}, k_{23}, \dots, k_{n0}, k_{n1}, k_{n2}, k_{n3}]$ represents the consequent parameters vector, n spindle speed, f_z feed per tooth, a_p depth of cut, $\overline{\omega}_i$ normalized firing strength and as output the arithmetic average of the roughness profile *Ra*.

Output of every fuzzy rule is connected with the output function defined by three different consequent parameters. It can be concluded from the foregoing that in training of the system 81 parameters are being adapted which then requires minimally 81 sets of input/output experimental data for the training of the FIS for assessing surface roughness. In addition to the training phase, the input/output experimental data are necessary for the checking phase too. For the checking phase 10 % of input/output experimental data are to be provided.

3. Results and discussion

Fig. 2 shows a machined sample. The arithmetic average of the roughness profile *Ra* is measured according to the standard ISO 4288 by means of a portable surface roughness tester produced by Taylor & Hobson model Surtronic S128.

The arithmetic average of the roughness profile *Ra* is measured on mid part of samples (between two white horizontal lines) as shown in Fig. 2 for each run separately. The upper and lower lines are 40 mm apart from the ends of the samples so that the central part width is 20 mm. The arithmetic average of the roughness profile *Ra* is measured vertically to the tangents of tool traces on the line where the tool traces are most apart, this line being at 10 mm distance from the left and the right edge of the sample and is parallel with them. For the measuring data processing the Talyprofile software produced by Taylor & Hobson is applied, designed to be used with the Surtronic series S-100 instruments.

After the experiment the acquisition of machined surfaces digital images of all samples was carried out using table scanner Scanjet 3100. The scanner optical resolution of 1200 points per inch was used to obtain greyscale image, i.e. image of the grey colour shades. For the greyscale image 8 bits per pixel were used while the grey colour shades values were represented in 256 levels.

After the acquisition all digital images are registered in matrix form from which input variables are quantified: greyscale mean value of all digital image matrix members, greyscale standard deviation of all digital image matrix members and the digital image matrix greyscale entropy that are, along with the measured arithmetic average of the roughness profile *Ra,* used as an input/output data base in creating the FIS for surface roughness assessing.

The greyscale mean value of digital image matrix is:

$$Mean = \frac{1}{N \times N} \sum_{x=1}^{N} \sum_{y=1}^{N} f(x,y) \tag{9}$$

where N presents the number of columns and number of rows of digital image, and $f(x,y)$ is a greyscale intensity value of the digital image matrix member defined by x and y.

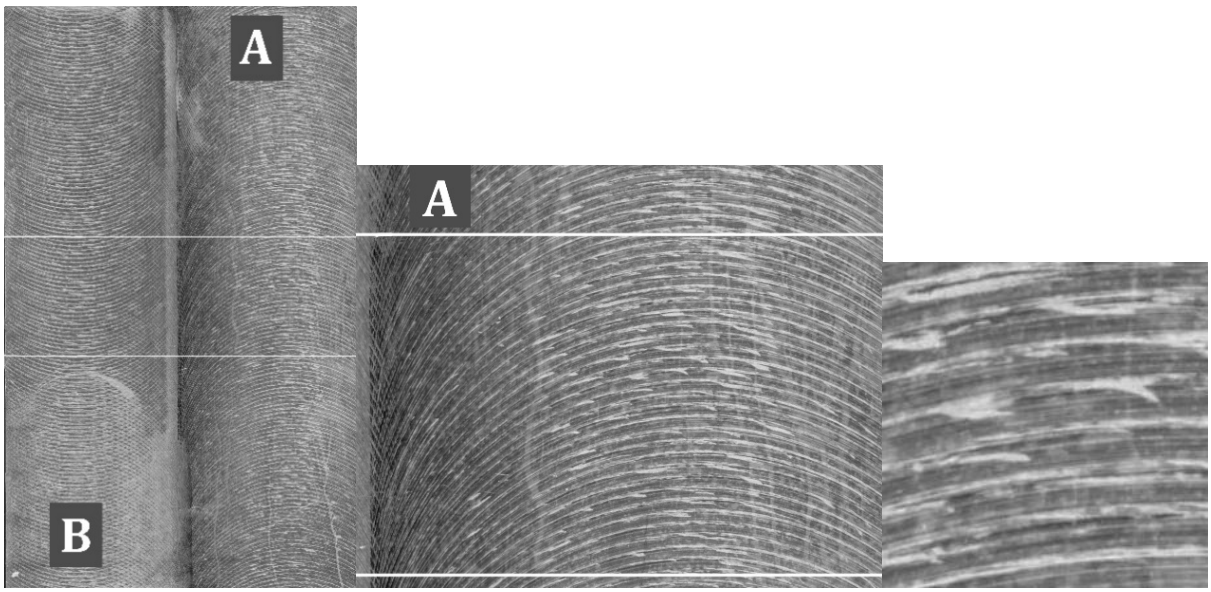

Fig. 2 Machined sample and roughness measuring points

The greyscale standard deviation of all digital image matrix members (N = 250) can be described as:

$$Std = \frac{1}{N}\sqrt{\sum_{x=1}^{N}\sum_{y=1}^{N}\left(f(x,y)-\bar{f}\right)^2} \tag{10}$$

where N presents the number of columns and number of rows of the digital image matrix, $f(x, y)$ is a greyscale intensity value of the digital image matrix defined by x and y while $\bar{f}$ is the digital image matrix mean greyscale value.

Entropy is a statistical measure of randomness that can be used to characterize the texture of the input image. The digital image matrix greyscale entropy is described as:

$$E = \sum_{i=1}^{256}(p_i \times \log_2 p_i) \tag{11}$$

where E is a scalar value representing the entropy of greyscale image I, and p is a vector which contains the histogram counts.

Resolution of all digital images used in this investigation was 250 × 250 pixels. The used resolution represents the size of the machined surface digital images denoting the place where the arithmetic average of the roughness profile *Ra* was measured along with the surrounding surface. The surface shown in the used digital images is between the white horizontal lines of the samples displayed in Fig. 2 for each run separately. To serve the needs of the current paper the digital images are used of those runs in which a higher value of the arithmetic average of the roughness profile *Ra* was measured. The digital image matrix consists of 250 rows and 250 columns.

Table 3 displays the extracted values of roughness (higher values Ra_{max} are displayed of two repeated measurements), and the earlier described input variables for creating the fuzzy inference system (mean greyscale value of all digital image matrix members, greyscale standard deviation of all digital image matrix members and the digital image greyscale matrix entropy).
The given data were used for generating FIS for assessing surface roughness using ANFIS. This system assesses the *Ra* values on the basis of the machined surfaces digital images and their features. The error of assessing i.e. of comparisons provided by the system with real values *Ra,* is expressed by the average normalized root mean square error (NRMSE). The assessing error of the fuzzy inference system created in this investigation is 0.0698 or 6.98 %.

The figures that follow demonstrate the arithmetic average of the roughness profile *Ra* dependence on greyscale standard deviation of all digital image matrix members and greyscale mean value of all digital image matrix members (Fig. 3), on entropy of digital image greyscale matrix and greyscale standard deviation of all digital image matrix members (Fig. 4), on entropy of digital image greyscale matrix and on the greyscale mean value of all digital image matrix members (Fig. 5).

The arithmetic average of the roughness profile *Ra* ranging from 0.194 μm to 1.68 μm has been measured in the experimental investigations. The measured outputs are ranged in four classes of surface roughness: N3 (from 0.1 μm to 0.2 μm), N4 (from 0.2 μm to 0.4 μm), N5 (from 0.4 μm to 0.8 μm), N6 (from 0.8 μm to 1.6 μm) and N7 (from 1.6 μm to 3.2 μm). The applicable parts of response surface in this particular case are given separately in Fig. 6.

It can be seen from Fig. 6 that slight changes in input variables have a considerable effect on output variable, the arithmetic average of the roughness profile *Ra*.

Table 3 Extracted values of roughness depending on technological parameters of machining, and the digital image values of variables for creating the fuzzy inference system

STD	RUN	Feed per tooth, mm/tooth	Bench feed, mm/min	Spindle speed, rev/min	Depth of cut, mm	$Ra_{\max,}$ μm	Greyscale mean value	Greyscale standard deviation	Greyscale matrix entropy
1	99	0.175	2450	3500	2	0.236	201.3327	12.9087	5.7077
2	32	0.1	800	2000	2	0.194	215.8912	14.4114	5.8688
3	40	0.25	3500	3500	2	0.340	216.4442	10.9891	5.4273
4	22	0.25	6500	6500	1	0.325	211.9918	14.9249	5.8883
5	34	0.25	2000	2000	2	0.291	211.6711	18.7212	6.2131
6	92	0.1	800	2000	2	0.259	207.0648	11.9313	5.6197
7	91	0.025	200	2000	2	0.295	205.5052	14.2197	5.8618
8	119	0.325	10400	8000	2	0.284	202.4441	21.4677	6.3535
9	112	0.25	6500	6500	2	0.892	172.1966	23.6160	6.5007
10	35	0.325	2600	2000	2	1.270	203.2657	26.0274	6,6797
11	6	0.4	3200	2000	1	1.050	181.5731	33.5879	7.0212
12	55	0.025	800	8000	2	0.549	200.8293	9.9470	5.3400
13	3	0.175	1400	2000	1	0.510	138.9439	30.9279	6.8194
14	96	0.4	3200	2000	2	1.300	192.3719	27.7303	6.7241
15	68	0.1	1400	3500	1	0.405	138.9501	18.3823	6.2209
16	16	0.25	5000	5000	1	0.845	146.9739	29.7534	6.8952
17	69	0.175	2450	3500	1	0.504	134.2705	27.7919	6.7490
18	115	0.025	800	8000	2	0.333	197.0068	8.3465	5.0556
19	11	0.325	4550	3500	1	0.755	124.9713	27.7997	6.6697
20	101	0.325	4550	3500	2	1.340	169.0206	24.9581	6.6209
21	54	0.4	10400	6500	2	1.560	175.4106	26.5330	6.5932
22	105	0.175	3500	5000	2	0.631	141.6713	18.3205	6.0764
23	30	0.4	12800	8000	1	1.030	149.9594	29.6730	6.8415
24	45	0.175	3500	5000	2	0.462	139.8943	19.5561	6.1107
25	77	0.325	6500	5000	1	0.684	142.7332	23.7919	6.5355
26	60	0.4	12800	8000	2	1.680	171.5458	25.1323	6.5677
27	113	0.325	8450	6500	2	1.660	150.6172	23.1638	6.5385
28	74	0.1	2000	5000	1	0.413	142.7963	19.5778	6.2314
29	78	0.4	8000	5000	1	1.040	149.5937	21.4949	6.4195
30	72	0.4	5600	3500	1	1.310	149.2047	21.1949	6.4186
31	62	0.1	800	2000	1	0.408	146.4589	17.7637	6.0372
32	70	0.25	3500	3500	1	0.742	159.4245	25.2728	6.5954
33	107	0.325	6500	5000	2	1.570	157.0338	26.5375	6.7189
34	51	0.175	4550	6500	2	0.359	142.6573	22.1164	6.4169
35	33	0.175	1400	2000	2	0.417	155.2297	20.8527	6.3764
36	7	0.025	350	3500	1	0.459	197.1356	8.5898	5.0740
37	86	0.1	3200	8000	1	0.376	150.2156	20.6194	6.3526
38	103	0.025	500	5000	2	0.342	216.3073	10.3385	5.3718
39	38	0.1	1400	3500	2	0.526	166.4716	21.4820	6.4444
40	100	0.25	3500	3500	2	1.140	164.7204	33.5821	7.0123
41	58	0.25	8000	8000	2	1.270	177.2273	29.6023	6.8859
42	76	0.25	5000	5000	1	0.802	157.8756	26.7976	6.6881
43	81	0.175	4550	6500	1	0.521	134.4788	22.0851	6.3085
44	89	0.325	10400	8000	1	0.761	152.5526	20.9315	6.3611
45	42	0.4	5600	3500	2	1.210	167.3245	21.3705	6.4070
46	28	0.25	8000	8000	1	0.855	145.4409	25.8796	6.5799
47	17	0.325	6500	5000	1	0.812	147.7410	20.9663	6.4149
48	41	0.325	4550	3500	2	1.540	171.2488	20.8178	6.3214
49	120	0.4	12800	8000	2	1.470	156.4950	21.1037	6.4185
50	47	0.325	6500	5000	2	1.090	176.9611	27.9537	6.8013
51	111	0.175	4550	6500	2	0.470	140.2953	20.8329	6.3067
52	98	0.1	1400	3500	2	0.374	145.4403	24.1626	6.4329
53	80	0.1	2600	6500	1	0.399	162.8991	21.2284	6.3343
54	14	0.1	2000	5000	1	0.366	154.3155	19.6337	6.2506
55	46	0.25	5000	5000	2	1.040	176.2519	32.7465	6.9622
56	56	0.1	3200	8000	2	0.364	155.8688	17.3140	6.0190
57	63	0.175	1400	2000	1	0.597	153.3269	29.7856	6.8004
58	104	0.1	2000	5000	2	0.386	159.6362	20.5342	6.2324
59	93	0.175	1400	2000	2	0.422	165.1706	23.2286	6.4068
60	117	0.175	5600	8000	2	0.508	149.4792	19.4560	6.0821

Table 3 Extracted values of roughness depending on technological parameters of machining, and the digital image values of variables for creating the fuzzy inference system (continuation)

STD	RUN	Feed per tooth, mm/tooth	Bench feed, mm/min	Spindle speed, rev/min	Depth of cut, mm	$Ra_{\max,}$ μm	Greyscale mean value	Greyscale standard deviation	Greyscale matrix entropy
61	8	0.1	1400	3500	1	0.402	156.5143	28.9983	6.7787
62	67	0.025	350	3500	1	0.463	224.1073	11.3163	5.4469
63	84	0.4	10400	6500	1	0.977	151.3250	27.0345	6.6960
64	90	0.4	12800	8000	1	0.945	155.1779	25.9010	6.6127
65	97	0.025	350	3500	2	0.202	218.8573	11.8558	5.5605
66	83	0.325	8450	6500	1	0.666	154.6065	27.3491	6.7255
67	59	0.325	10400	8000	2	1.300	152.1983	24.2644	6.5952
68	106	0.25	5000	5000	2	1.150	157.4970	30.3303	6.7487
69	79	0.025	650	6500	1	0.336	174.5179	16.0944	5.9967
70	5	0.325	2600	2000	1	0.778	152.4728	23.3246	6.5248
71	48	0.4	8000	5000	2	1.600	163.3946	25.3079	6.6660
72	108	0.4	8000	5000	2	1.560	158.2985	19.6642	6.2761
73	53	0.325	8450	6500	2	1.460	176.6186	27.1825	6.7422
74	29	0.325	10400	8000	1	0.715	173.9498	23.3387	6.5550
75	21	0.175	4550	6500	1	0.513	157.2126	25.0313	6.5654
76	25	0.025	800	8000	1	0.257	194.3272	17.8550	6.0991
77	52	0.25	6500	6500	2	1.500	176.9590	34.1330	7.0064
78	109	0.025	650	6500	2	0.510	215.7320	7.6283	4.9336
79	37	0.025	350	3500	2	0.264	184.7601	12.6105	5.6820
80	64	0.25	2000	2000	1	0.932	164.4880	23.3275	6.4361
81	31	0.025	200	2000	2	0.326	196.8387	9.8417	5.3327
82	49	0.025	650	6500	2	0.277	196.4967	18.2400	6.1901
83	27	0.175	5600	8000	1	0.418	180.7377	30.4711	6.7616
84	110	0.1	2600	6500	2	0.319	194.5997	16.2075	6.0494
85	61	0.025	200	2000	1	0.449	202.4482	12.0212	5.6169
86	88	0.25	8000	8000	1	0.345	208.5057	18.1894	6.2054
87	50	0.1	2600	6500	2	0.362	216.7653	12.7031	5.6936
88	87	0.175	5600	8000	1	0.315	203.7227	16.5828	6.0807
89	26	0.1	3200	8000	1	0.377	204.2278	17.9229	6.1923
90	43	0.025	500	5000	2	0.322	225.7510	4.8023	4.3056
91	94	0.25	2000	2000	2	0.391	185.6580	17.7899	6.1080
92	19	0.025	650	6500	1	0.412	226.0397	4.4847	4.2012
93	102	0.4	5600	3500	2	0.657	193.8495	17.3608	6.1385
94	44	0.1	2000	5000	2	0.302	205.5300	15.0375	5.9108
95	15	0.175	3500	5000	1	0.317	198.4703	17.8107	6.1613
96	73	0.025	500	5000	1	0.361	217.4270	5.6124	4.5311
97	1	0.025	200	2000	1	0.404	210.2537	11.3657	5.5270
98	36	0.4	3200	2000	2	0.652	183.9130	18.6225	6.1525
99	116	0.1	3200	8000	2	0.371	210.2263	13.8650	5.8338
100	82	0.25	6500	6500	1	0.359	194.8133	13.8527	5.8269
101	71	0.325	4550	3500	1	0.454	179.7367	21.4364	6.3853
102	23	0.325	8450	6500	1	0.413	200.2917	16.8814	6.0965
103	65	0.325	2600	2000	1	0.550	183.4905	18.8896	6.2459
104	2	0.1	800	2000	1	0.371	220.3295	13.6538	5.8036
105	114	0.4	10400	6500	2	0.561	185.6083	18.8118	6.2636
106	4	0.25	2000	2000	1	0.369	201.7676	15.8028	6.0238
107	18	0.4	8000	5000	1	0.544	186.0058	22.0295	6.4740
108	85	0.025	800	8000	1	0.408	219.5023	5.5210	4.4854
109	75	0.175	3500	5000	1	0.347	187.1892	15.5448	5.9636
110	24	0.4	10400	6500	1	0.529	205.4299	15.7066	6.0073
111	95	0.325	2600	2000	2	0.557	176.9512	21.9477	6.4261
112	39	0.175	2450	3500	2	0.336	190.3445	19.2155	6.2940
113	13	0.025	500	5000	1	0.415	225.9157	5.7998	4.5690
114	9	0.175	2450	3500	1	0.323	188.4408	17.3426	6.1525
115	66	0.4	3200	2000	1	0.566	182.2851	19.7799	6.3321
116	20	0.1	2600	6500	1	0.378	218.3453	12.7629	5.6885
117	57	0.175	5600	8000	2	0.332	186.9872	18.1653	6.2152
118	10	0.25	3500	3500	1	0.356	189.2162	16.7248	6.1067
119	12	0.4	5600	3500	1	0.495	184.4284	19.5615	6.3077
120	118	0.25	8000	8000	2	0.321	192.7420	17.5391	6.1643

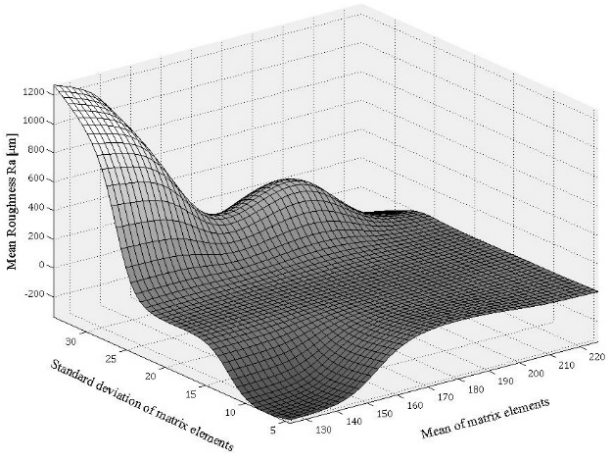

Fig. 3 Dependence of *Ra* on standard deviation and mean value of digital image matrix members

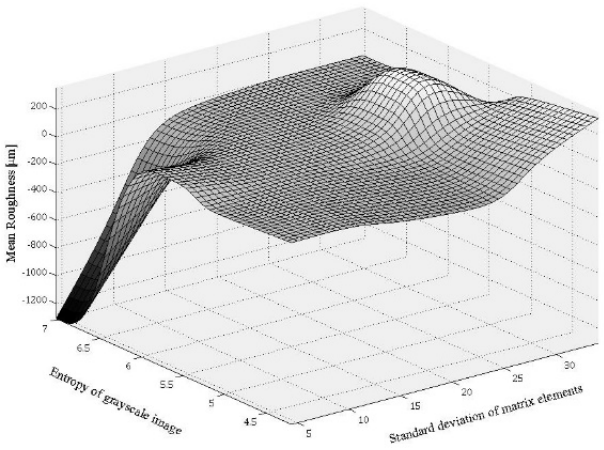

Fig. 4 Dependence of *Ra* on entropy and standard deviation of digital image matrix members

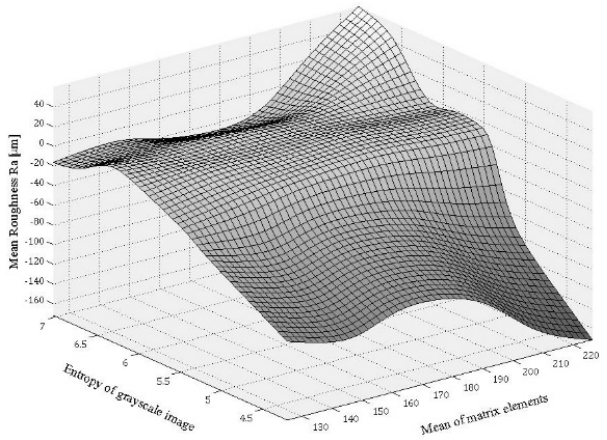

Fig. 5 Dependence of *Ra* on entropy and mean value of digital image matrix members

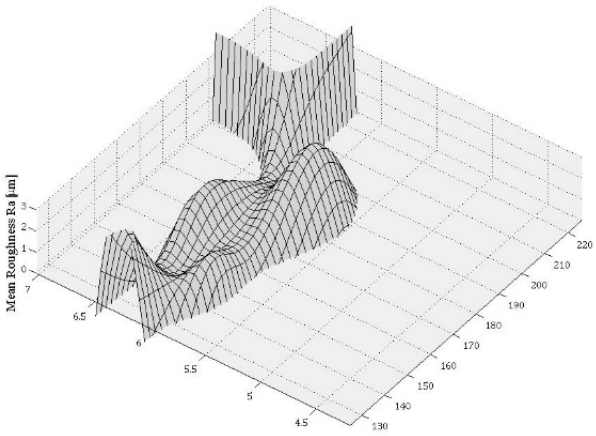

Fig. 6 Applicable part of the response surface shown in Fig. 5

It can be seen from the papers that deal with assessing the roughness of machined surfaces on the basis of the features of digital image that the range of measured roughness has a great impact on the level of error assessing. The wider the range of measured roughness, with the uniform distribution by the roughness classes, the lower the error of assessment. The error of assessment in this study (6.98 %) was significantly influenced by outlier values. Specifically, almost 97 % of the measured values of roughness belong to the roughness classes N4, N5 and N6. The remaining values and part of roughness values in class N6 are outliers. Without outliers the error of assessment of the machined surface roughness is expected to be significantly lower.

4. Conclusion

The conducted investigation is part of a project whose ultimate objective is to build an online system for machined surface roughness monitoring i.e. roughness monitoring in real time. The system should faster carry out the activities of required control of machined surfaces, testing would be cheaper, and monitoring during machining would help to timely react to possible deviations and to reduce subsequent costs. The investigations in this paper are focused on assessing the machined surface roughness based on the features of digital image with the use of adaptive neuro-fuzzy inference system (ANFIS). A controlled parameter of surface roughness is the arithmetic average of the roughness profile *Ra*. The following features of digital image are studied in the paper: mean greyscale values of all digital image matrix members, standard greyscale deviation of all digital image matrix members and entropy of digital image greyscale matrix. Comparison of real values *Ra* and the values provided by the built system is shown by the nor-

malized root mean square error (NRMSE), or assessing error. The conducted investigation enters the area of high speed machining. Therefore the machined surfaces are of high quality and the measured roughness is very small. Thus the features of digital images become quite similar and a higher assessing error is expected. The fuzzy inference system obtained in the present investigation has an assessing error of 6.98 %. However, even with such an error, the technical requirements set on the workpiece as regards quality of machining, should not be diminished.

The plan is to expand the research on existing material, but also conduct research on other materials. This would be a way to expand the base of digital photos and their features and to accumulate sufficient knowledge to influence the reduction of assessing errors.

Acknowledgement

This research is accomplished within the projects Nos. IZIP-2014-95 and INGI-2015-28 financed by the Josip Juraj Strossmayer University of Osijek.

References

[1] Stankovic, I., Perinic, M., Jurkovic, Z., Mandic, V., Maricic, S. (2012). Usage of neural network for the prediction of surface roughness after the roller burnishing, *Metalurgija*, Vol. 51, No. 2, 207-210.
[2] Simunovic, K., Simunovic, G., Saric, T. (2015). Single and multiple goal optimization of structural steel face milling process considering different methods of cooling/lubricating, *Journal of Cleaner Production*, Vol. 94, 321-329, doi: 10.1016/j.jclepro.2015.02.015.
[3] Zuperl, U., Cus, F. (2015). Simulation and visual control of chip size for constant surface roughness, *International Journal of Simulation Modelling*, Vol. 14, No. 3, 392-403, doi: 10.2507/IJSIMM14(3)2.282.
[4] Vukelic, D., Tadic, B., Miljanic, D., Budak, I., Todorovic, P.M., Randjelovic, S., Jeremic, B.M. (2012). Novel workpiece clamping method for increased machining performance, *Tehnički vjesnik – Technical Gazette*, Vol. 19, No. 4, 837-846.
[5] Brezocnik, M., Kovacic, M., Ficko, M. (2004). Prediction of surface roughness with genetic programming, *Journal of Materials Processing Technology*, Vol. 157-158, 28-36, doi: 10.1016/j.jmatprotec.2004.09.004.
[6] Pare, V., Agnihotri, G., Krishna, C. (2015). Selection of optimum process parameters in high speed CNC end-milling of composite materials using meta heuristic techniques – A comparative study, *Strojniški vestnik – Journal of Mechanical Engineering*, Vol. 61, No. 2, 176-186, doi: 10.5545/sv-jme.2014.1914.
[7] Simunovic, G., Simunovic, K., Saric, T. (2013). Modelling and simulation of surface roughness in face milling, *International Journal of Simulation Modelling*, Vol. 12, No. 3, 141-153, doi: 10.2507/IJSIMM12(3)1.219.
[8] Çolak, O. (2014). Optimization of machining performance in high-pressure assisted turning of Ti6Al4V alloy, *Strojniški vestnik – Journal of Mechanical Engineering*, Vol. 60, No. 10, 675-681, doi: 10.5545/sv-jme.2014.1914.
[9] Nammi, S., Ramamoorthy, B. (2014). Effect of surface lay in the surface roughness evaluation using machine vision, *Optik – International Journal for Light and Electron Optics,* Vol. 125, No. 15, 3954-3960, doi: 10.1016/j.ijleo.2014.01.152.
[10] Klancnik, S., Ficko, M., Balic J., Pahole, I. (2015). Computer vision-based approach to end mill tool monitoring, *International Journal of Simulation Modelling*, Vol. 14, No. 4, 571-583, doi: 10.2507/IJSIMM14(4)1.301.
[11] Krolczyk, G., Raos, P., Legutko, S. (2014). Experimental analysis of surface roughness and surface texture of machined and fused deposition modelled parts, *Tehnički vjesnik – Technical Gazette,* Vol. 21, No. 1, 217-221.
[12] Samtaş, G. (2014). Measurement and evaluation of surface roughness based on optic system using image processing and artificial neural network, *The International Journal of Advanced Manufacturing Technology*, Vol. 73, No. 1, 353-364, doi: 10.1007/s00170-014-5828-1.
[13] Stępień, K., Makiela, W., Stoić, A., Samardžić, I. (2015). Defining the criteria to select the wavelet type for the assessment of surface quality, *Tehnički vjesnik – Technical Gazette,* Vol. 22, No. 3, 781-784, doi: 10.17559/TV-20140124110406.
[14] Lee, K.C., Ho, S.J., Ho, S.Y. (2005). Accurate estimation of surface roughness from texture features of the surface image using an adaptive neuro-fuzzy inference system, *Precision Engineering*, Vol. 29, No. 1, 95-100, doi: 10.1016/j.precisioneng.2004. 05.002.
[15] Jeyapoovan, T., Murugan, M. (2013). Surface roughness classification using image processing, *Measurement*, Vol. 46, No. 7, 2065-2072, doi: 10.1016/j.measurement.2013.03.014.
[16] Morala-Argüello, P., Barreiro, J., Alegre, E. (2012). A evaluation of surface roughness classes by computer vision using wavelet transform in the frequency domain, *The International Journal of Advanced Manufacturing Technology,* Vol. 59, No. 1, 213-220, doi: 10.1007/s00170-011-3480-6.
[17] Palani, S., Natarajan, U. (2011). Prediction of surface roughness in CNC end milling by machine vision system using artificial neural network based on 2D Fourier transform, *The International Journal of Advanced Manufacturing Technology,* Vol. 54, No. 9, 1033-1042, doi: 10.1007/s00170-010-3018-3.

[18] Ho, S.Y., Lee, K.C., Chen, S.S., Ho, S.J. (2002). Accurate modeling and prediction of surface roughness by computer vision in turning operations using an adaptive neuro-fuzzy inference system, *International Journal of Machine Tools and Manufacture*, Vol. 42, No. 13, 1441-1446, doi: 10.1016/S0890-6955(02)00078-0.
[19] Palani, S., Natarajan, U., Chellamalai, M. (2013). On-line prediction of micro-turning multi-response variables by machine vision system using adaptive neuro-fuzzy inference system (ANFIS), *Machine Vision and Applications*, Vol. 24, No. 1, 19-32, doi: 10.1007/s00138-011-0378-0.
[20] Natarajan, U., Palani, S., Anandampilai, B. (2012). Prediction of surface roughness in milling by machine vision using ANFIS, *Computer-Aided Design & Applications*, Vol. 9, No. 3, 269-288, doi: 10.3722/cadaps.2012.269-288.
[21] Jeyapoovan, T., Murugan, M. (2013). Surface roughness classification using image processing, *Measurement*, Vol. 46, No. 7, 2065-2072, doi: 10.1016/j.measurement.2013.03.014.
[22] Zawada-Tomkiewicz, A. (2010). Estimation of surface roughness parameter based on machined surface image, *Metrology and Measurement Systems*, Vol. 17, No. 3, 493-504.
[23] Priya, P., Ramamoorthy, B. (2007). The influence of component inclination on surface finish evaluation using digital image processing, *International Journal of Machine Tools and Manufacture*, Vol. 47, No. 3-4, 570-579, doi: 10.1016/j.ijmachtools.2006.05.005.
[24] Lee, B.Y., Yu, S.F., Juan, H. (2004). The model of surface roughness inspection by vision system in turning, *Mechatronics*, Vol. 14, No. 1, 129-141, doi: 10.1016/S0957-4158(02)00096-X.
[25] Gadelmawla, E.S., Al-Mufadi, F.A., Al-Aboodi, A.S. (2014). Calculation of the machining time of cutting tools from captured images of machined parts using image texture features, *Proceedings of the Institution of Mechanical Engineers, Part B: Journal of Engineering Manufacture*, Vol. 228, No. 2, 203-214, doi: 10.1177/0954405413481291.
[26] Dutta, S., Datta, A., Das Chakladar, N., Pal, S.K., Mukhopadhyay, S., Sen, R. (2012). Detection of tool condition from the turned surface images using an accurate grey level co-occurrence technique, *Precision Engineering*, Vol. 36, No. 3, 458-466, doi: 10.1016/j.precisioneng.2012.02.004.
[27] Shahabi, H.H., Ratnam, M.M. (2009). In-cycle monitoring of tool nose wear and surface roughness of turned parts using machine vision, *The International Journal of Advanced Manufacturing Technology*, Vol. 40, No. 11, 1148-1157, doi: 10.1007/s00170-008-1430-8.
[28] Nathan, D., Thanigaiyarasu, G., Vani, K. (2014). Study on the relationship between surface roughness of AA6061 alloy end milling and image texture features of milled surface, *Procedia Engineering*, Vol. 97, 150-157, doi: 10.1016/j.proeng.2014.12.236.
[29] Kamguem, R., Tahan, S.A., Songmene, V. (2013). Evaluation of machined part surface roughness using image texture gradient factor, *International Journal of Precision Engineering and Manufacturing*, Vol. 14, No. 2, 183-190, doi: 10.1007/s12541-013-0026-x.